ROYAL SOCIETY OF CHEMISTRY

Journal Name

ARTICLE

Linker-free covalent immobilization of nisin using atmospheric pressure plasma induced grafting

Jenny Aveyard[a], James W. Bradley*[a], Kirsty McKay[a], Fiona McBride[b], David Donaghy[a], Rasmita Raval[b] and Raechelle A. D'Sa*[c]

The linker-free covalent immobilization of polymers on surfaces has the potential to impart new properties and functions to surfaces for a wide range of applications. However, most current methods for the production of these surfaces involve multiple chemical steps and do not have a high degree of control over the chemical functionalities at the surface. A comprehensive study detailing the facile two-step covalent grafting of the antimicrobial peptide nisin to polystyrene surfaces is reported. Functionalization is achieved using an atmospheric pressure plasma jet and the reaction is monitored and compared with a standard wet chemical functionalization approach using a variety of analytical techniques. The reactive species produced by the atmospheric pressure plasma jet were analyzed by mass spectrometry and optical emission spectroscopy. The surface chemistry and topography of the functionalized surfaces were analyzed using contact angle measurements, Fourier infrared spectrophotometry (FTIR), X-ray photoelectron spectroscopy and atomic force microscopy respectively. Following surface analysis, the antimicrobial efficacy of the covalently grafted nisin against two major food borne pathogens (*Staphylococcus aureus and Listeria monocytogenes*) was assessed at two different pHs. Results demonstrated that a post-plasma treatment step after nisin deposition is required to covalently graft the peptide to the surface. The covalent immobilization of nisin resulted in a significant reduction in bacterial counts within a short 30 minutes contact time. These surfaces were also significantly more antimicrobial to those prepared via a more traditional wet chemical approach indicating that the reported method could be a less expensive and time consuming alternative.

1.0 Introduction

The ability to design and fabricate surfaces and materials that are antimicrobial is of great importance various industries. Once bacteria adhere to a solid surface, they form microcolonies and subsequently become embedded within a polysaccharide matrix forming a biofilm, which is extremely difficult to remove. A number of strategies have been employed in the quest for effective antimicrobial surfaces including adhesion resistance, contact killing and biocide leaching.[1, 2] Adhesion resistant or non-fouling surfaces typically have hydrophilic macromonomers such as poly(ethylene glycol) immobilized on the surface which prevent the initial adhesion of planktonic bacteria[3, 4]. This "first generation" strategy is a passive approach that is effective only if the architecture of the grafted polymers on the surface is cohesive and forms the requisite structure with water to make it unfavourable for bacteria to adhere. The other two strategies (biocide leaching and contact killing) involve bactericidal surfaces which are able to disrupt the cell on contact, causing cell death[5-7] In some instances, an antibacterial surface may exhibit both antifouling and bactericidal characteristics.[8] Biocide leaching surfaces

release cytotoxic compounds such as silver or copper that are able to intercept bacteria in their vicinity[6, 7]. While these types of surfaces are highly effective, there is evidence to suggest that high concentrations of these ions can potentially have cytotoxic effects. Furthermore, the duration and effectiveness of the antimicrobial action of this release approach is limited by loading and release kinetics. The contact killing strategy involves either chemical modifications to tether an antimicrobial agent onto the surface[9-11] or physical modifications which in general involve mimicking naturally antimicrobial topographies such as shark skin or cicada wings[5, 12]. The contact killing strategy offers the most promising avenue to developing antimicrobial surfaces as it kills bacteria on contact.

Antimicrobial peptides (AMPs) are an innate part of the immune response that are produced by all complex organisms and are effective against a broad range of Gram negative and Gram positive bacteria, including those resistant to established antibiotic drug therapies and mycobacteria, enveloped viruses, parasites and fungi.[13-15] As such the immobilization of AMPs represents a promising new generation of biomimetic antimicrobial surfaces. Nisin is extremely versatile as an AMP due to its diverse applications in many fields from medicine to the food industry. It is active at relatively low concentrations against Gram positive pathogens such as *Staphylococcus aureus, Listeria monocytogenes, Bacillus cereus* and *Clostridium perfringens.*[16] Nisin has been used as a food preservative in the dairy industry for over 40 years, it is non-toxic, heat stable, odourless and has been approved by the Food and Drug

a. Department of Electrical Engineering and Electronics, University of Liverpool, L69 3GJ, UK. Email: jbradley@liverpool.ac.uk
b. The Open Innovation Hub for Antimicrobial Surfaces, Surface Science Research Centre, Department of Chemistry, University of Liverpool, L69 3BX, UK.
c. Department of Mechanical, Materials and Aerospace Engineering, University of Liverpool, L69 3GH, UK. Email: r.dsa@liverpool.ac.uk

Administration (FDA). Nisin is a cationic amphiphilic peptide consisting of 34 amino acids with a cluster of hydrophobic residues at the N-terminus and hydrophilic residues at the C-terminus (Figure 1). The mechanism of action of nisin is based on its ability to disrupt the bacterial cell membrane.[17, 18]

Several methods exist for the attachment of nisin, and other AMPs to surfaces such as low density polyethylene (LDPE)[19, 20] and stainless steel[9, 11, 21, 22] but they often involve time-consuming wet chemical protocols with expensive reagents or rely on the electrostatic adhesion of the peptides which could be unstable and liable to leaching. The covalent attachment of AMPs to surfaces allows for longevity of antimicrobial activity due to a higher concentration of appropriately structured peptides in one location.[10, 23, 24] Covalent immobilization is however, not often straightforward as most biomaterials are designed to be non-reactive, thereby rarely presenting the functionality required for such bioconjugation reactions. The immobilization of a biomolecule requires reliable attachment and sufficient density to allow it to interact preferentially with bacteria. Furthermore, covalently immobilized nisin needs to be robust for a long period of time without delaminating, while being presented in an active conformation. Several research groups have studied the effects of AMP immobilization on its antimicrobial activity using traditional wet chemical methodologies based on linker chemistries.[10, 24] The difficulty of translating linker-chemistries include the complexity of wet chemical reactions, side reactions, inconsistent yields and possible toxicity issues.
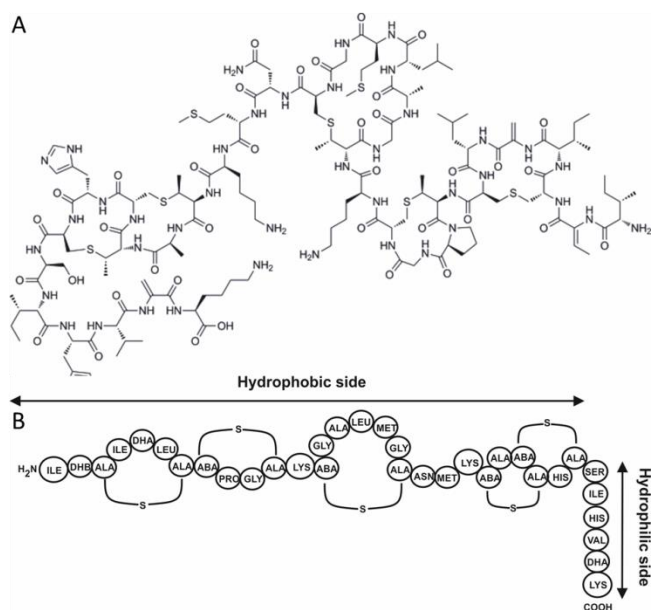

Figure 1: A) Chemical and B) primary structure of nisin

Plasma-based approaches for functionalizing surfaces, in particular those used for biomolecule immobilization[25-29], are a promising alternative to wet chemical approaches.[30-33] Plasma-assisted modification can be used to modify a wide range of substrates and by controlling the processing parameters, the plasma environment can be used for surface nano-structuring, chemical activation, and the deposition of biologically active and passive coatings. The majority of studies in this regard use plasma-treated surfaces or plasma polymers as interfacial

bonding layers for the subsequent permanent immobilization of molecules designed to elicit specific biological responses.[31-33] Our group and a few others have studied the feasibility of plasma or radiation for inducing the grafting of polymers/biomolecules of interest. These include the plasma/radiation grafting for antimicrobial/antifouling polymers such as poly(ethylene oxide) (PEO)[34-37] and polyamines[38-40] for antifouling/antimicrobial applications. Plasma induced grafting has the potential to covalently immobilize molecules of interest with efficiency and simplicity and would provide a significant advancement in bioconjugation research. The advantage of this technique is manifested in terms of financial cost, ease of integration, and scalability of potential modification techniques. Furthermore, the advantages of using an atmospheric pressure plasma system for the covalent immobilization are: (1) atmospheric pressure plasma combines both UV and ion bombardment without the engineering costs associated with a vacuum system; (2) atmospheric pressure plasmas produces discharges with a low breakdown voltage, uniform density of charged species and high concentrations of ions and radicals; and, (3) properties of the polymer phase is controllable.[41]

The primary goal of this study is to investigate the utility of an in house built atmospheric pressure plasma jet to *in situ* graft nisin onto polystyrene and to determine the conditions necessary for the retaining of antimicrobial efficacy. This method of plasma induced grafting was compared to the traditionally used method of using plasma polymer coatings that contain reactive chemical groups useful for the subsequent covalent immobilization by wet chemical reactions. The chemistry of the plasma jet was analyzed using mass spectrometry and optical emission spectroscopy and substrates were characterized before and after functionalization using contact angle measurements, Fourier infrared spectroscopy (FTIR), X-ray photoelectron spectroscopy (XPS) and atomic force microscopy (AFM). The antibacterial efficacy of the immobilized nisin against gram positive bacterium *Staphylococcus aureus* and *Listeria monocytogenes* was determined by bacterial assays performed at two different pH's.

2.0 EXPERIMENTAL SECTION

2.1 Materials
All chemicals were of the highest grade available and were purchased from Sigma Aldrich. Sheets of polystyrene (PS), 1.2 mm thick (Goodfellow, UK) were used as the substrate materials. Samples were cleaned by sonication in ethanol for 15 min and dried under a laminar flow hood.

2.2 Atmospheric pressure plasma jet (APPJ)
The plasma jet consisted of a 12 cm long glass tube (outer diameter (OD) of 4 mm inner diameter (ID) of 2.4 mm) with a copper ring electrode attached 1.5 cm from the end of the capillary. The plasma jet was powered using a kHz sinusoidal power source. The power supply consisted of a digital function generator (TG2000, AIM-TTI Instruments) driving a commercial audio amplifier (HQ power, VPA2350MB). A voltage step-up transformer (Express Transformers, UK) was connected at the output to generate the required high voltages for discharge breakdown. The peak-to-peak voltage was fixed to 7 kV and the frequency was 20 kHz (the wave was symmetrical). The capillary tube was fed with pure He (99.996%) at a flow rate of 1 standard

litre per minute (SLM). The helium outflow was able to interact with the ambient laboratory air as it passed from the capillary exit to the substrate.   The substrate was mounted on an automated 2D stage (Thor Labs) to allow full control of the plasma jet. The distance between the capillary tube and the PS sample during plasma processing is 5 mm. A schematic diagram of the experimental setup and photograph of the jet (inset) is shown in Figure 2.

Table 1: Nomenclature of various surfaces

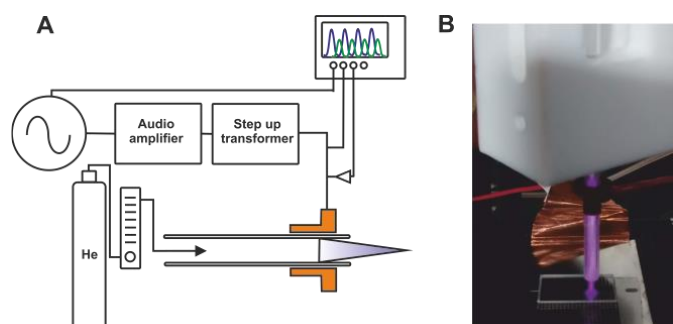| Substrate	Experimental Conditions			
	Reaction Path	Pre-treated	Post-treated	Conc. Nisin (mg ml^{-1})
PS	Control	N	N	0
PS_{ox}	Control	Y	N	0
PS_{oxNis1}	Control	Y	N	1
PS_{oxNis2}	Control	Y	N	2
PS_{oxNis5}	Control	Y	N	5
PS-g-Nis$_1$	A	Y	Y	1
PS-g-Nis$_2$	A	Y	Y	2
PS-g-Nis$_5$	A	Y	Y	5
$PS_{EDC/NHS}$	B	Y	N	2
PS_{Nis2}	Control	N	N	2

Figure 2: A) Schematic of APPJ setup B) Photograph of APPJ in operation

2.3 Analysis of Atmospheric pressure He plasma jet by mass spectrometry

Mass spectrometry was used to analyze the species produced in the He plasma jet. The mass spectrometer was a quadrupole-based (QMS) molecular beam mass spectrometer (MBMS), (HPR-60; Hiden Analytical Ltd, UK). It consists of a three stage differentially pumped inlet system separated by aligned skimmer cones and turbomolecular pumps. The three pressure reduction stages, provide a pressure reduction from atmospheric pressure to 10^{-1} Torr, 10^{-5} Torr and 10^{-7} Torr.[42]

The HPR-60 can be used to detect neutral species (RGA mode) as well as both positive and negative ions (SIMS mode). In RGA mode the neutral molecular beam is internally ionized before it reaches the quadrupole stage. In SIMS mode the molecular beam is already ionized and positive and negative ions are separated by applying voltages to the skimmer cones. To reduce chances of modifying the plasma chemistry internally the mass spectrometer was fitted with a small extraction orifice (100 μm), decreasing the likelihood of electric field and plasma sheath penetration into the low-pressure region. The presence
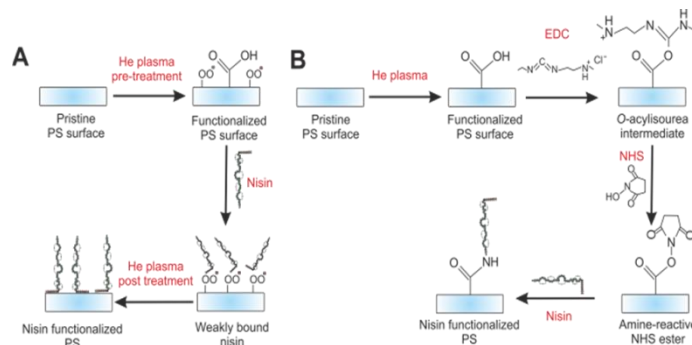

Figure 3: A) Grafting of nisin onto plasma treated PS. B) Reaction scheme detailing the attachment of nisin on plasma treated, EDC/NHS ester functionalized PS.

of the mass spectrometer orifice and extraction cone inherently perturbs the plasma; however, this is thought to be similar to the perturbation experienced when the plasma is in direct contact with a surface. The plasma jet was positioned 5 mm from the sampling orifice and analysis of neutral species (RGA mode) and positive/negative ions (SIMS mode) produced by the jet, and by the interaction of the jet with ambient air were performed.

2.4 Optical spectroscopy analysis of the He plasma jet

Optical emission spectroscopy (Ocean optics, US) was also used to analyze the reactive species produced in the He plasma jet. The optical fibre was positioned orthogonal to jet axis at a 0.5 cm distance from the plume. Spectra were collected in the range of 200-900 nm over a period of 5 minutes with an integration time of 1000 ms.

2.5 Grafting of antimicrobial nisin on PS

The nisin peptides were immobilized onto the plasma functionalized surfaces by two methodologies as per Figure 3. Pathway A involves functionalization of PS with the plasma jet, dip coating the substrates in nisin followed by plasma induced grafting of nisin. Pathway B involves plasma polymerization of acetic acid on the PS followed by carbodiimide-mediated immobilization of nisin. The nomenclature of the different surfaces are presented in Table 1.

2.6 Plasma induced grafting of nisin on PS (Pathway A)

PS substrates (2 cm x 1 cm; Goodfellow, Cambridge Ltd) were first sonicated in pure isopropanol for 280 s, rinsed in fresh isopropanol and then dried in a stream of N_2. PS was then oxidatively functionalized by scanning the He plasma jet across the surface for a total of 450 s (PS_{ox}). At the end of this time, 80 μl of nisin (1, 2 or 5 mg ml-1 in 0.01 M acetic acid) was deposited on the PS and the surface was post treated by scanning the He plasma jet across the surface as before (PS-g-Nis$_x$). After treatment, PS substrates were washed thoroughly in acetic acid and deionized water then dried in a stream of nitrogen. Control substrates either did not contain nisin (PS or plasma treated PS) or were not pre/post treated with plasma before or after nisin deposition. All substrates were stored in a desiccator for at least two days before any surface analysis or bacterial tests were performed.

2.7 Grafting of nisin onto PS using carbodiimide mediated chemistry (Pathway B)

PS substrates were oxidatively functionalized by scanning a He plasma jet across the surface as described above. Treated PS was then immersed in a solution of 0.1 M 2-(N-morpholino)ethanesulfonic acid buffer (MES) containing 0.05 M N-hydroxysuccinimide (NHS) and 0.2 M 1-Ethyl-3-(3-dimethylaminopropyl) carbodiimide hydrochloride (EDC) for 3 hours. At the end of this time, substrates were washed thoroughly in MES buffer and then were immersed in nisin solution (2 mg ml-1 in 0.01 M acetic acid) for 3 hours. Following the reaction with nisin, substrates were washed thoroughly with MES buffer and deionized water and then dried under a stream of nitrogen.

2.8 Contact angle measurement

Water contact angle (WCA) measurements were obtained with a contact angle meter (CAM 100, KSV instruments) by depositing a droplet (0.2 µl) of degassed deionized water onto the centre of the substrates. The drop shape analysis software calculated the WCA using curve fitting based on the Young-Laplace equation and had an inaccuracy of +/- 0.1 degrees. Three measurements in different areas of each substrate were taken.

2.9 FTIR Analysis

FTIR spectra were obtained with a FT/IR 4100 fitted with a MIRacle ATR accessory (Pike Technologies, US). Cleaned PS was used as a blank and spectra were acquired over a 500 - 3000 cm^{-1} wavelength range and analyzed with Spectra Manager Version II software (Jasco Corp, UK).

2.10 XPS Analysis

The XPS data were taken on an Axis-Supra instrument (Kratos Analytical, UK) using monochromatic Al Kα radiation (225 W) and a low-energy electron flood source for charge compensation. Survey scan spectra were acquired using a pass energy of 160 eV and a 1 eV step size. Narrow region scans were acquired using a pass energy of 20 eV and a 0.1 eV step size. The hybrid lens mode was used in both cases. The samples were attached to the sample bar using BeCu plates and screws. The data were converted into the VAMAS file format (*.vms) and imported into the CasaXPS version 2.3.12 (Casa software, UK) software package for analysis. Quantitative analysis of the spectral data was obtained after subtraction of a linear background and calculation of the peak area for the most intense spectral line for each elemental species detected to determine the relative atomic percentage concentration (at.%). The resultant data are reported as average values ±2 standard deviations. All C 1s peaks were recalibrated so that the peak maximum appeared at a binding energy of 285.0 eV.

2.11 AFM Analysis

AFM was used to any monitor any topographical changes to the PS surface during functionalization. A Bruker Multimode 8 fitted with NanoScope controller operating in ScanAsyst mode was used with a silicon tip and a cantilever operating at a scan rate of 0.9 Hz. Images had a resolution of 512 x 512 pixels and were analyzed using Nanoscope analysis software. Zero order plane fitting and zero order flattening were used to correct any errors that occurred during the imaging process. The average roughness (Ra) and root-mean-squared roughness (Rq) was measured from the analysis of the images at 3 µm x 3 µm scan size using WSxM 5.0 Develop 8.2 software (WSxM solutions).[43]

2.12- Bacterial culture and growth conditions.

The antimicrobial tests were carried out against *S. aureus* and *L. monocytogenes*. Pre-cultures were prepared by inoculating 10 ml of nutrient broth (NB) with a single bacterial colony. After overnight incubation at 37°C, 100 µl of pre-culture was added to 10 ml of NB and the culture was incubated overnight. At the end of this time the culture was diluted with NB to obtain an optical density (OD) of 0.1 for the bacterial tests.

2.13- Antimicrobial activity of nisin functionalized PS

The antimicrobial activity of the functionalized PS was tested using previously reported protocols.[34] Pre-cultures of *S. aureus* and *L. monocytogenes* were prepared as described above and then the optical density of the culture was adjusted to 0.1 at 600 nm. The concentration of both species of bacteria incubated with the substrates in all experiments was 1 x 10^8 CFU/ml. For the acidic pH experiments, the pH of the NB used to dilute the culture was adjusted to pH 5.5 (using 0.01 M HCl). PS substrates were placed in sterile 6 well plates and 2 ml of bacterial cell suspension was added into each well. The samples were then incubated at 37 °C for 30 min to allow adhesion to take place. At the end of this time, non-adherent bacteria were removed by washing the substrates 3 times in phosphate buffered saline (PBS, pH 7.4 experiment) or MES (pH 5.5 experiment) and then the substrates were transferred to universals containing 10 cm^3 sterile PBS (or MES) and sonicated for 10 min. After sonication, the appropriate dilution was plated onto agar plate and incubated at 37 °C overnight. The bacterial response was determined by plotting the percentage reduction of cultivable cells versus the experimental condition. Longer timepoints up to 6 hours was evaluated, however, no difference in percent reduction in bacterial adhesion was seen after 30 min; therefore this time point was chosen as the incubation time to carry out the antimicrobial analysis. All samples were run in triplicate and repeated twice.

2.14 -Statistical analysis

The statistical analysis for both the antimicrobial data was performed with Origin® (v. 9, OriginLab Corp., USA). One way analysis of variance (ANOVA) was used to compare mean values in order to determine equivalence of variance between pairs of samples. Significance between groups was determined using the Bonferroni multiple comparison test. A value of $p < 0.05$ was taken as statistically significant. Results are reported as means ± 1 standard deviation.

3.0 Results

The experimental strategy undertaken in this paper is shown in Figure 3. PS surfaces are plasma treated by an in house built APPJ which provided a defined wetting property of the surface onto which a nisin solution can be applied.[44] Without this plasma pretreatment condition insufficient wetting might lead to inhomogeneous coating of the peptide on the surface. Nisin is drop cast on the plasma treated polystyrene and covalently grafted using carbodiimide mediated chemistry and plasma induced grafting (Path A and B in Figure 3).

3.1 APPJ Analysis

In the first step, the APPJ generates reactive species that are transferred to the polymer surface through a flux of neutral particles, electrons, ions and radicals, as well as from exposure to UV radiation. Mass spectrometry (MS) and optical emission spectroscopy (OES) analysis have been used to analyze the reactive species generated in the plasma for the pretreatment and grafting steps.
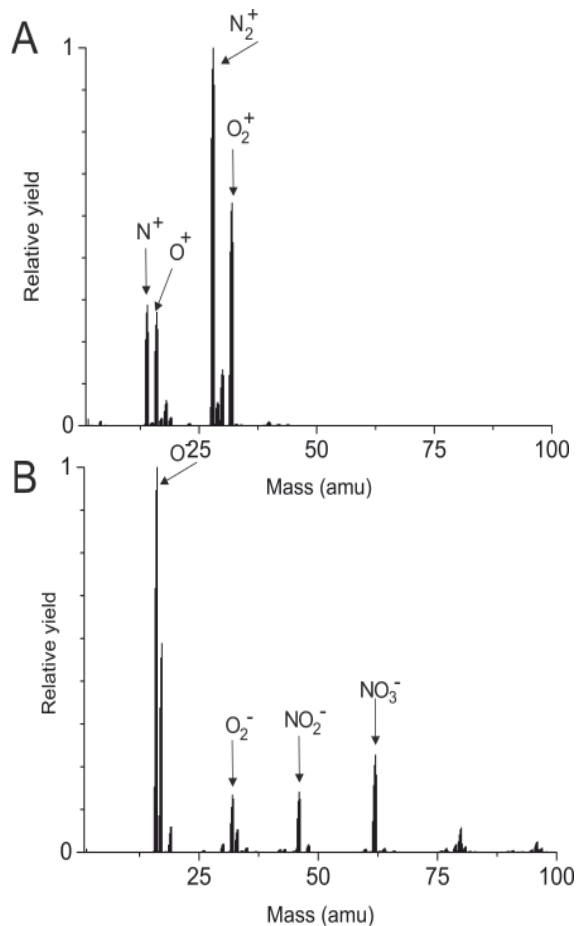

Figure 4: A) MS detailing the relative yield of positive ions obtained with the He APPJ focused on the mass spectrometer orifice B) MS detailing the relative yield of negative ions obtained with the He APPJ focused on the mass spectrometer orifice.

3.1.1- Mass spectrometry analysis of the He plasma jet

MS was used to analyze the composition of the He APPJ and confirm the presence of reactive species capable of grafting the peptide to the PS surface. The relative positive and negative ion yields obtained can be seen in the mass spectrum presented in Figure 4 A and B. With plasma jets operating at atmospheric pressure, the composition of the jet is influenced by the interaction of the He stream with the surrounding air. The dominant positive ions detected in the plasma were N^+, O^+, N_2^+ and O_2^+. These species are predominately produced through dissociation and Penning ionization reactions with helium metastable species. The dominant negative ions were O^-, O_2^-, NO_2^- and NO_3^-. These are produced predominately through dissociation and electron attachment reactions. These results are consistent with those previously reported by McKay et al[45].
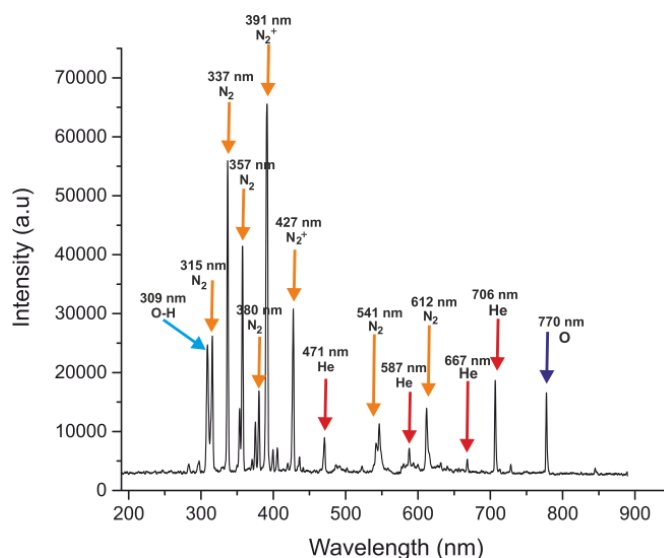

Figure 5: Optical emission spectra of He atmospheric pressure plasma jet. The optical fibre was positioned 0.5 cm from the centre of the jet plume. Nitrogen species peaks are labelled orange, helium peaks are in red, oxygen in purple and hydroxyl in blue

3.1.2- Optical emission spectroscopy analysis of the He plasma jet

OES was used to identify the chemically reactive species that were present in the He jet plume with the results given in Figure 5. The emission spectra in the plasma jet is composed of an OH transition at 308 nm, formed from interactions of the plume with water vapor present in the ambient air; He I transition $3d3D \rightarrow 2p3P0$ at 587.6 nm, He I transition $3d1D \rightarrow 2p1P0$ at 667.8 nm, He I transition $3s3S1 \rightarrow 2p3P0$ at 706.5 nm; O I transition $3p5P \rightarrow 3s5S0$ at 777.41 nm. Second positive series emission bands of the N_2 molecule (C $3\Pi_u \rightarrow$ B $3\Pi^g$) between 300-400 nm and first positive series emission bands (C $3\Pi^g \rightarrow$ A3 Σ_u+) at 540 nm. The first-negative series of N2+ (B2 Σ_u+$\rightarrow$ X2 Σ^g+) were observed at 391 and 427 nm.[46, 47]

## 3.2 Surface Analysis

3.2.1 Static Contact Angle

The wettability of the PS substrates before and after treatment was determined by measuring the static contact angle. The results shown in Table 2 indicate that the contact angle decreases from 93.7° on the native PS surface to 45.5° on the plasma treated PS (PS_{ox}). No further decrease in the contact angle was observed after nisin was either covalently (PS_{-g-Nis}) or electrostatically (PS_{oxNis}) adsorbed onto the surface. The contact angle of the PS_{Nis2} surface is 61.0°, which indicates that while nisin has adhered onto untreated PS, it may have adhered in a different conformation, perhaps as a result of denaturation due to poor wetting of the untreated surface.

Table 2. Contact angles of the PS substrates. Measurements expressed as an average value ± the standard deviation.

Substrate	Conditions	
	Reaction Path	Contact angle
PS	Control	93.7 ± 1.6
PS_{ox}	Control	45.5 ± 1.5
PS_{oxNis1}	Control	45.0 ± 2.9
PS_{oxNis2}	Control	47.7 ± 1.7
PS_{oxNis5}	Control	49.2 ± 2.1
$PS\text{-}g\text{-}Nis_1$	A	49.5 ± 0.7
$PS\text{-}g\text{-}Nis_2$	A	48.2 ± 1.4
$PS\text{-}g\text{-}Nis_5$	A	47.0 ± 1.1
$PS_{EDC/NHS}$	B	42.5 ± 1.1
PS_{Nis2}	Control	61.0 ± 5.0

3.2.2- FTIR analysis

FTIR was used to monitor any chemical changes during each step in the reaction pathways. The spectra of PS_{ox}, PS_{Nis2}, $PS\text{-}g\text{-}Nis_2$ is given in Figure 6. Atmospheric pressure plasma treatment of PS results in oxidative functionalization as observed in the appearance of the characteristic carbonyl peak observed at 1730 cm^{-1}. The presence of nisin on the PS_{Nis2} and $PS\text{-}g\text{-}Nis_2$ samples is confirmed with peaks appearing at 1550 cm^{-1} (N-H bending, amide II), 3200 cm^{-1} (NH stretching) and 1650 cm^{-1} (C=O stretching, amide I) as seen in Figure 5. The absence of these peaks in the sample that has not been post plasma treated after nisin deposition (PS_{Nis2}) suggests that there is a low concentration of nisin absorbed on the surface of the PS, which is not observable by the detection limit of the FTIR. [48, 49]
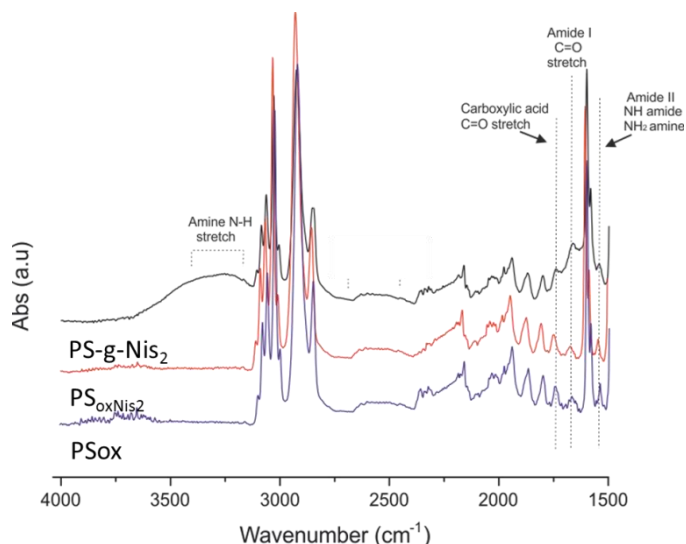
Figure 6: FTIR spectra of PS_{ox} (blue), PS_{Nis2} (red) and $PS\text{-}g\text{-}Nis_2$ (black).

3.2.3- XPS analysis

XPS was used to confirm the success of each step of the process. The elemental composition and the high resolution C1s data given in Tables 3 and 4, respectively. As pristine PS has no oxygen in its structure, oxidation of the surface by the plasma process can be accurately quantified post-treatment (Tables 3 and 4). Pristine PS contains the expected aromatic and aliphatic C–C/C–H peaks centered at 285.0 eV and the characteristic π–π* shake up satellite peak at 292.0 eV (Table 3). Curve fitting of the corresponding C 1s envelope of PS_{ox} (Table 3) indicates new contributions to the polymer surface from components at C–O (286.5 eV), C-O/C-N (287.5 eV), O=C–O/ O=C–N (289.0 eV). Immobilization of nisin onto PS by both paths is confirmed by the appearance of a nitrogen moiety (between 1% and 3.5%, Table 4). The C1s spectra of the nisin grafted surfaces also clearly show a characteristic peptide O=C–N at 289.0 eV, confirming nisin has adhered on the surface as opposed to possible adventitious contaminants. All of these results represent vigorously washed sample surfaces to confirm the covalent grafting of the peptide onto PS. Nisin adsorbs onto a hydrophobic untreated PS as well, with an at. % N concentration of 2.5 %.

Table 3. XPS derived elemental at. % for the different surface treatments

Substrate	at. %		
	C	N	O
PS	98.60	0	1.40
PS_{ox}	94.87	0	5.13
PS_{oxNis1}	84.10	3.47	11.61
PS_{oxNis2}	83.69	3.25	12.71
PS_{oxNis5}	82.59	3.52	13.64
$PS\text{-}g\text{-}Nis_1$	86.30	1.04	12.66
$PS\text{-}g\text{-}Nis_2$	85.65	2.61	11.74
$PS\text{-}g\text{-}Nis_5$	80.72	2.84	16.44
$PS_{EDC/NHS}$	83.15	3.53	12.04
PS_{Nis2}	89.25	2.45	8.30

Table 4. XPS derived at. % for the contributions to the deconvoluted C 1s spectral envelope for the different surface treatments

Substrate	at. % C 1s			
	C-C /C-H	C-O/ C-N	O=C-O/O=C-N	π-π*
PS	94.71	0	0	5.29
PS_{ox}	81.77	12.76	0	5.47
PS_{oxNis1}	77.70	19.46	0	2.84
PS_{oxNis2}	79.88	16.69	0	3.43
PS_{oxNis5}	69.63	27.68	0	2.69
$PS\text{-}g\text{-}Nis_1$	69.01	26.27	0	4.73
$PS\text{-}g\text{-}Nis_2$	73.06	23.64	0	3.30
$PS\text{-}g\text{-}Nis_5$	62.71	25.83	8.64	2.82
$PS_{EDC/NHS}$	50.70	41.08	4.71	3.51
PS_{Nis2}	85.60	10.80	0	3.59

3.2.4 AFM analysis

The surface topography of PS, PS_{ox} and PS_{oxNis}, PS-g-Nis surfaces created via Pathway A were determined by AFM analysis. Representative images are presented in Figure 7. The untreated PS surface was relatively smooth (Ra=4.48 nm) and there was only a slight increase in surface roughness (Ra=5.07 nm) when the surface was oxidized with the APPJ (PS_{ox}). This demonstrates that under the conditions used, little or no etching of the surface occurs. We have previously shown that PS preferentially undergoes oxygen functionalization rather than chain scission reactions with plasma treatment. [50]   When nisin is electrostatically adsorbed (PS_{oxNis}), there
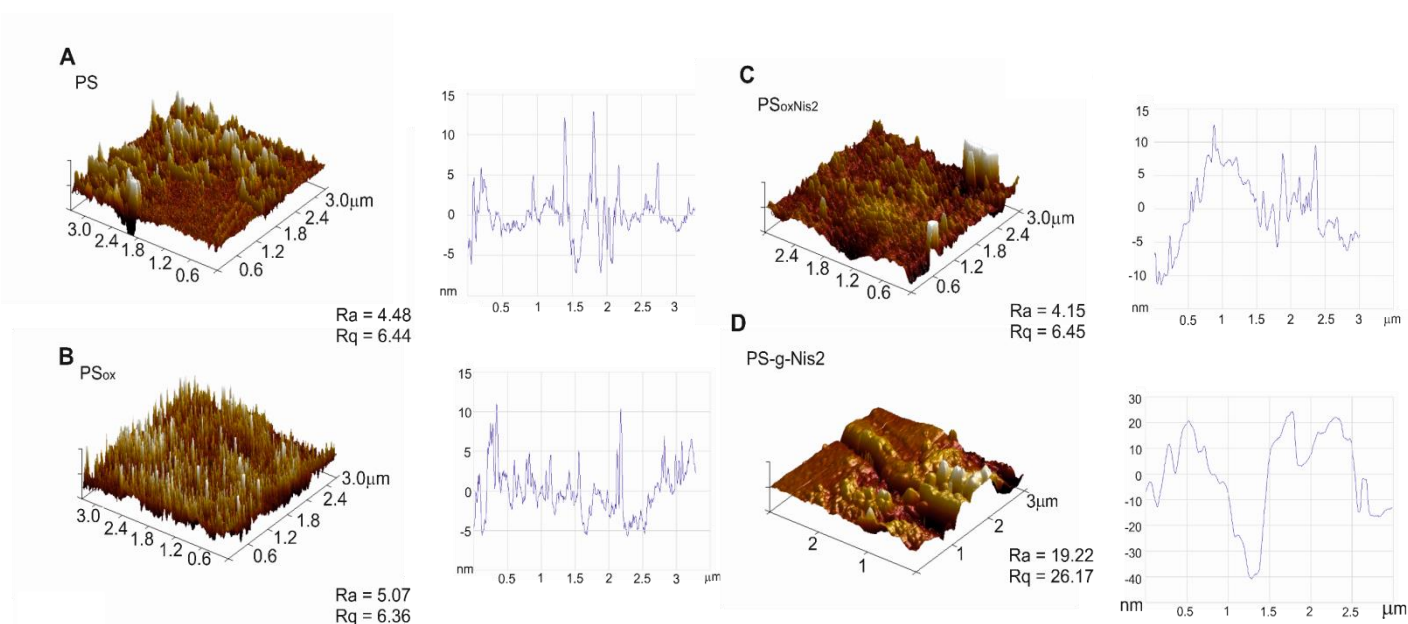
Figure 7: AFM height mode images of various samples at 3x3 μm^{2}size A) Pristine PS, B) PS$_{ox}$, C) PS$_{oxNis2}$ and D) PS-g-Nis$_2$.

is a slight decrease in the surface roughness (Ra=4.15 nm) which suggests that the underlying topography of the substrate is maintained and the nisin molecules are most likely horizontally adhered onto surface. When nisin is covalently grafted onto the PS surface (PS-g-Nis) an increase in both height and surface roughness (Ra=19.22 nm) is observed. This is indicative of multiple layers of nisin orientated perpendicular to the surface. These results are consistent with those reported by Karam *et al.* who also observed an increase in surface roughness and height when nisin was absorbed in a perpendicular orientation on a smooth hydrophilic surface.[16]

3.3 Antimicrobial response

The antimicrobial activity of immobilized nisin was tested against two species of bacteria, *S. aureus* and *L. monocytogenes* at pH 5.5 and 7.4 (Figures 6 and 7 respectively). These two pHs were chosen because nisin has been reported to have an enhanced effect at pH 5.5 compared with that 7.4.[51, 52] This has been ascribed to the fact that nisin is more stable at a lower pH; whereas at neutral and alkaline pHs, nisin is unstable and insoluble.[53] There was a reduction in antimicrobial activity against both bacterial species at both pHs when the substrates were not post treated with the APPJ after nisin deposition indicating that nisin needs to be covalently immobilized to be a more effective antimicrobial surface. This result is in agreement with Choquet and coworkers who observed a decrease in the amount of non-covalently bound nisin on surfaces after washing with PBS.[9] In this work, we observed a more pronounced reduction in the antimicrobial activity at pH 5.5, suggesting that acidic incubation and washing conditions during the bacterial tests were more effective in dissociating any weakly bound nisin. At both pH 7.4 and 5.5, there is a statistically significant (p<0.05) increase in antimicrobial activity when nisin is covalently grafted rather than electrostatically adsorbed onto the surfaces for both bacterial species.

There is also a statistically significant (p< 0.05) increase in the antimicrobial activity as the amount of nisin on these substrates is increased from 1 mg mL^{-1} to 2 mg mL^{-1}. No further increase in activity is observed at 5 mg mL^{-1} suggesting that higher concentrations may lead to steric hindrance and that higher densities of immobilized peptides may not be able to penetrate the bacterial cell wall as efficiently or that grafting of the peptides has reached saturation at 2 mg mL^{-1}. From Figures 8 and 9, it is clear that there is a reduction in antibacterial activity against *L. monocytogenes* at pH 7.4 compared with pH 5.5 which is consistent with previous reports of nisin's increased activity at more acidic pHs. This reduction in activity is not observed for *S. aureus* indicating that differences in antimicrobial activity are a function of bacterial species. Interestingly, the plasma induced grafted surfaces showed a statistically significant (p< 0.05) increase in antimicrobial activity in comparison to the wet chemical modification method.
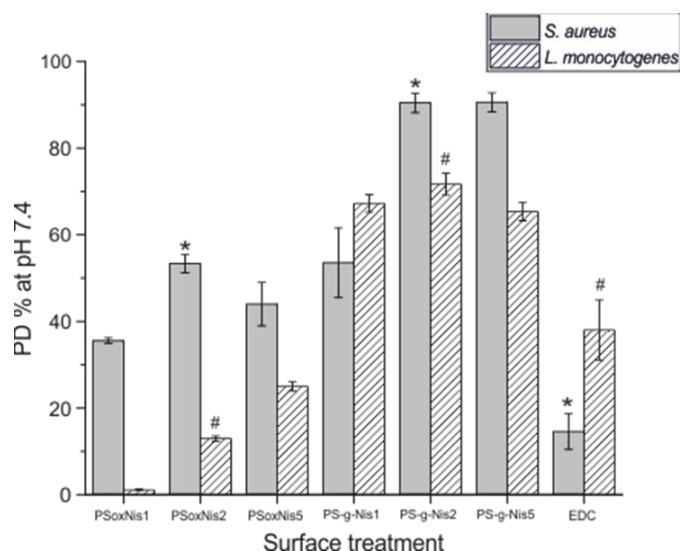
Figure 8: The percent reduction of *S. aureus* and *L. monocytogenes* adhering after 30 min of incubation on the variously modified PS at pH 7.4. *Indicates statistically significant differences with $p < 0.05$ between PS-g-Nis$_2$ and PS$_{oxNis2}$, EDC surfaces for *S. aureus*. # Indicates statistically significant differences with $p < 0.05$ between PS-g-Nis$_2$ and PS$_{oxNis2}$, EDC surfaces for *L. monocytogenes*.
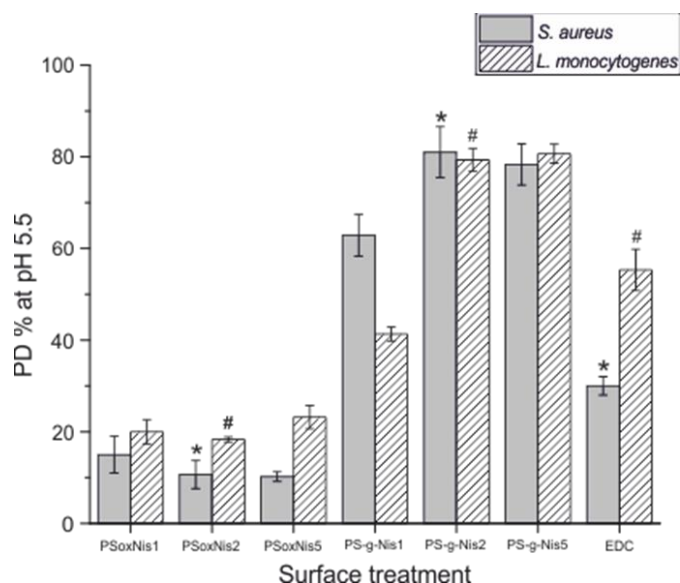

Figure 9: The percent reduction of *S. aurues* and *L. monocytogenes* adhering after 30 min of incubation on the variously modified PS at pH 5.5. *Indicates statistically significant differences with $p < 0.05$ between PS-g-Nis$_2$ and PS$_{oxNis2}$, EDC surfaces for *S. aureus*. # Indicates statistically significant differences with $p < 0.05$ between PS-g-Nis$_2$ and PS$_{oxNis2}$, EDC surfaces for *L. monocytogenes*.

4. Discussion

4.1 Orientation of grafted nisin

Nisin is a cationic amphiphilic peptide consisting of 34 amino acids with a cluster of hydrophobic residues at the N-terminus and hydrophilic residues at the C-terminus (Figure 1). The mechanism action of nisin is based on its ability to disrupt the bacterial cell membrane. The initial interaction is electrostatic between the positive regions of the peptide and the negatively charged bacterial cell membrane. [17, 18] The N-terminus of nisin interacts with lipid II, an integral cell wall precursor, permeabilizing the membrane and inhibiting cell wall synthesis, subsequently resulting in cell death.[17, 18] Owing to nature of the bactericidal mechanism, it is of utmost importance to understand the orientation, structure and charge of the peptide tethered onto a surface.
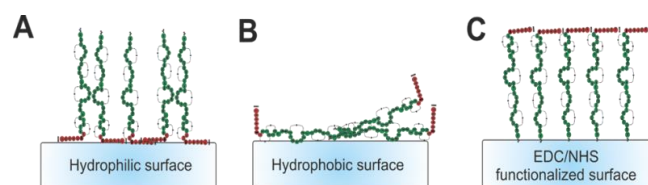

Figure 10: Proposed orientation of nisin on surfaces. A) The amine group at the N- terminus binds to the NHS functionalized surface. The hydrophobic region may be sterically hindered and unable associate efficiently with the bacterial cell membrane. B) The hydrophobic region of the nisin binds to the hydrophobic surface. The number of hydrophobic regions available to interact with the bacterial cell membrane is reduced. C) The hydrophilic region of nisin binds to the hydrophilic surface and the hydrophobic region is free to interact with the bacterial cell membrane.

The orientation of nisin on a variety of hydrophobic and hydrophilic surfaces has been much debated.[20, 54, 55] It is generally accepted that on hydrophilic substrates the hydrophilic domain of the nisin is orientated towards the substrate (Figure 10A) whereas on a hydrophobic substrate the reverse occurs (Figure 10 B). Bower *et al* observed that multiple layers of nisin absorbed to silanized hydrophobic silica surfaces but these layers were easily eluted by washing in buffer or could be displaced by other proteins.[55] They also noted that despite the adsorption of higher concentrations of nisin on the hydrophobic surface, the antibacterial activity was significantly reduced. It was concluded that nisin undergoes a conformational change upon adsorption which inhibited interaction with the bacterial cell membrane. Chihib *et al* also observed reduced antibacterial activity of nisin when adsorbed to hydrophobic low-density polyethylene (LDPE) compared with hydrophilic plasma treated acrylic acid coated LDPE.[19, 20] In both of these studies, however, nisin is just physisorbed onto the surfaces and susceptible to leaching.

In 2013, Choquet *et al* used a two-step method to covalently attach EDC/NHS functionalized nisin to plasma activated aminosilanized stainless steel (Figure 11A).[9] In 2014, the same authors reversed the wet chemical approach, by now functionalizing stainless steel with vinyltrimethoxysilane, maleic anhydride and EDC/NHS.[21] Nisin was then attached to the surface *via* an amide bond formed between the amino functionality on the peptide and the EDC/NHS functionalized surface (Figure 11B). Each of these immobilization approaches would result in a different nisin orientation of nisin, thereby affecting the antimicrobial efficacy. Theoretically, the former approach would result in a more favourable peptide orientation, with attachment of

the NHS functionalized hydrophilic residues to the aminosilanized substrate and the N-terminus of the peptide free to interact with the bacteria. However, it is also possible that the unmodified amine terminus of one nisin molecule could crosslink with another NHS functionalized nisin molecule (Figure 11C).   In this work, EDC/NHS functionalized PS surfaces were prepared in order to compare the plasma grafting method and absorption with the standard wet chemical covalent attachment method. Both the XPS and bacterial experiments confirm that nisin is attached, but the EDC/NHS functionalized substrates exhibited a lower antibacterial activity in comparison to ones prepared by the plasma grafting method. This suggests that the nisin may not be in the correct orientation or could be inhomogeneous on the surface.

4.2 Mechanism of grafting of nisin

The experimental strategy undertaken in this paper is shown in Figure 3. PS surfaces are plasma treated by an in-house built APPJ for the purpose of providing a defined wetting property conducive to the subsequent homogenous spreading of nisin on the surface.[44] Subsequent to this nisin, was grafted using plasma induced grafting (Pathway A) and a wet chemical approach (Pathway B). The wet chemical approach is used as a control to which the feasibility of the plasma induced grafting methodology is compared against.
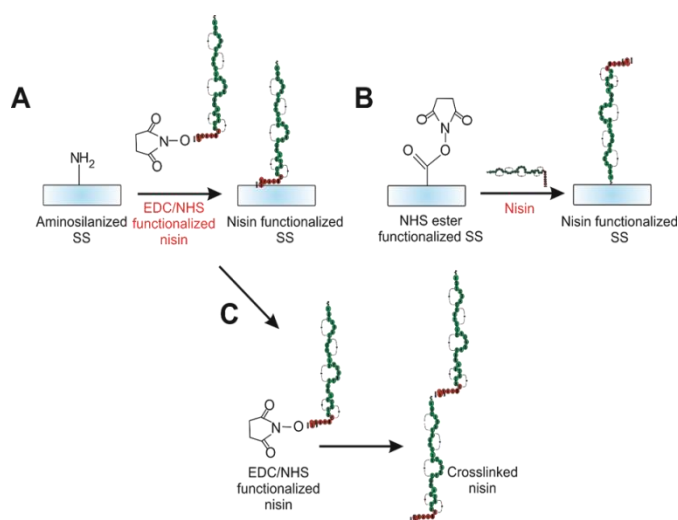

Figure 11: Schematic detailing nisin functionalization methods reported by Choquet *et al.*[9] A) Attachment of EDC/NHS functionalized nisin to aminosilanized stainless steel (SS) B) Attachment of unmodified nisin to EDC/NHS modified SS.[21]   C) Problem arising from method A. EDC/NHS chemistry is used to functionalize the carboxylic acid terminus of the peptide. As the amine terminus of the peptide is unmodified, it is free to react with other NHS functionalized nisin molecules.   This could lead to crosslinked nisin.

Pathway A involves plasma induced grafting of nisin onto plasma activated PS surfaces. Plasma processing is a widely used technique for surface functionalization prior to biomolecule immobilization. In most cases the energetic species created in the plasma break bonds generating free radicals at the surface and subsurface, which can subsequently crosslink or create functional groups such as C=O,

COOH and OH. The depth to which the radicals are created is determined by the energetics of the plasma and the penetration depth of the bombarding species.[26] For example argon creates a higher intensity of energy delivery to a shallower depth than hydrogen.[26] From the mass spectra and optical emission spectra, we have identified the main ions (O[-], O$_2$[-], NO$_2$[-], NO$_3$[-], N, O, N$_2$[+] and O$_2$[+]) and radicals (·OH, ·O). The APPJ results in the ions being accelerated directionally onto the substrate, which has a slightly negative potential compared with the plasma and will bombard untreated PS and the nisin coated PS. The free radicals generated by the plasma raise the surface energy making the surface more hydrophilic and assisting in retaining the native conformation of the immobilized peptide as also seen by Bilek and coworkers.[26, 56] Surface groups created by the plasma are generally unstable (referred to as "aging" or hydrophobic recovery) and therefore need to be used immediately after treatment.[57] As such, these plasma treated surfaces are used less frequently for immobilization reactions than plasma polymerized surfaces.[57] Consequently in this work a second plasma treatment step is used to generate energetic species that impinge on the substrate (PS) or onto nisin to allow for covalent binding.[44]

Bilek's group uses an energetic ion-assisted plasma process (plasma immersion ion implantation) to produce an activated surface to directly immobilize biomolecules covalently on the surfaces without a second treatment step. The covalent linkage forms as a result of the free radicals, oxygen-containing groups and unsaturated groups (that are stable for months[58]) on the polymeric substrate with the side chain groups in the proteins.[25, 26, 58, 59] The methodology used applies very high voltages (several kilovolts) and requires specialized apparatus rather than using a conventional plasma system and therefore their plasma-derived surfaces group do not have the same aging profile as seen by us and others which prevents direct covalent binding. [28, 60]

Gogolides and coworkers have shown that plasma treated surfaces suffer from progressive aging, which negatively affects subsequent biomolecule immobilization.[28] To circumvent this, they introduce a short annealing step after plasma treatment in order to induce accelerated hydrophobic recovery and preserve the chemical functionality (especially of carboxyl groups) created by the plasma to then ensue biomolecule immobilization. They have shown that plasma generated carboxyl or carbonyl groups can form a covalent linkage with a pendant amino via an unstable Schiff base intermediate. They compare this direct method of immobilization to that with EDC/NHS activation and find that without the carbodiimide crosslinker, protein immobilization occurs mainly through a combination of physical adsorption and covalent binding. Using EDC/NHS activation enables the carboxyl groups present on the surface to form stable amide bonds with the proteins, as evidenced from the higher amount of protein remaining after rigorous washing to non-activated surfaces. Our results agree with that of Gogolides; APPJ treatment of PS results in the generation of the radicals which are not as long lived as those observed by Bilek and therefore, do not instigate direct covalent immobilization of nisin onto PS. Rather, nisin that is adsorbed onto surfaces after plasma treatment is perhaps physically and chemically attached as seen by Gogolides.[28]

ARTICLE Journal Name

While Gogolides uses annealing to accelerate the hydrophobic recovery, we plasma treat the physisorbed nisin to covalently graft it onto the surface. Therefore, immobilization of nisin most likely proceeds via (1) peroxy/alkoxy or stabilized carbon centered radicals on the polymer substrate add to the vinyl (C═C) group of the nisin, (2) the formation of a stabilized allylic radical on the peptide which can recombine with active radicals on the substrate surface or (3) recombination of surface/subsurface radicals with radicals on the peptide. We have previously reported a similar mechanism for grafting of poly(ethyleneglycol) methacrylate onto polymer surfaces.[34-36] In a similar vein, this type of plasma/radiation grafting has been previously reported for grafting antimicrobial/antifouling polymers such as poly(ethylene oxide) (PEO)[34-37] and polyamines polyamines[38-40] for antifouling/antimicrobial applications. The necessity for a second energetic step was also reported by Barbucci *et al.* who have shown that photo-immobilization was necessary for the linker-free covalent binding of hyaluronan on plasma activated polyethylene-terephthalate (PET).[27] This same group used H_2 plasma-pretreated polyethylene films to graft oxygen-containing polar chemical functionalities which were used as anchor groups for the surface immobilization of the antimicrobial enzyme lysozyme.[29] They have previously shown that H_2 cross-linking pre-treatments were necessary to obtain a better PE surface which was less prone to ageing in air for hydrophobic recovery.[61] The cross-linking of the PE topmost layers is due to internal chain rearrangements after H abstraction, UV radiations, and ion bombardment and is analogous to Gogolides[28] strategy of annealing the polymer surfaces.

4.3 Tethering nisin with linker chemistry

In this work Pathway B was carried out via a traditional wet chemical methodology using a carbodiimide-mediated bioconjugation reaction to form an amide bond between a carboxylic acid and an amine group. Carbodiimide coupling has often been considered favourably because it can be performed in buffered aqueous solution and thus avoids the need for reaction conditions that could denature proteins. Carbodiimide can form an unstable acyliourea intermediate that can undergo a side reaction to a stable acylurea, which is why succinimide is usually used in conjunction as it generates a stable succinimidyl ester which has a limited lifetime of ~20 min.[62] The carbodimiide reaction can theoretically proceed in two ways: (1) covalent linking is with a carboxyl group on the surface and an amine group on the peptide (Figure 11B) and (2) activate carboxyl groups on the protein react them with amine groups on the surface (Figure 11A). A major problem with the second approach is that activated carboxyl groups can react with amine groups on the same or another peptide, thus achieving crosslinking rather than surface immobilization as seen in Figure 11C. Crosslinked multimers can precipitate onto surfaces and covalent grafting might be erroneously assumed.[63] As such we have used the former method to graft nisin onto our surfaces. Both the XPS and bacterial experiments confirm that nisin is attached, but the EDC/NHS functionalized substrates exhibited a lower antimicrobial activity in comparison with the plasma grafting method. This suggests that the nisin may not be in the correct orientation or could be inhomogeneous on the surface when immobilized with EDC/NHS linker chemistry.

5.0 Conclusions

Although research has shown that EDC/NHS linker chemistry can be used with nisin to create stable antibacterial surfaces, the method is time-consuming (>2 hr) and involves multiple functionalization steps with costly reagents. Furthermore, plasma pre-treatment to activate/clean the surface is still required. Conversely, the plasma grafting method reported here takes approximately 15 minutes and does not require costly reagents and therefore is a promising new approach for the tethering of peptides onto surfaces that can be scaled up for industrial applications.

Acknowledgements

Notes and references

1. K. Vasilev, J. Cook and H. J. Griesser, *Expert Rev Med Dev*, 2009, **6**, 553-567.
2. J. A. Lichter, K. J. Van Vliet and M. F. Rubner, *Macromolecules*, 2009, **42**, 8573-8586.
3. I. Banerjee, R. C. Pangule and R. S. Kane, *Adv Mater*, 2011, **23**, 690-718.
4. S. Krishnan, C. J. Weinman and C. K. Ober, *J Mater Chem*, 2008, **18**, 3405-3413.
5. E. P. Ivanova, J. Hasan, H. K. Webb, V. K. Truong, G. S. Watson, J. A. Watson, V. A. Baulin, S. Pogodin, J. Y. Wang and M. J. Tobin, *Small*, 2012, **8**, 2489-2494.
6. C. E. Santo, E. W. Lam, C. G. Elowsky, D. Quaranta, D. W. Domaille, C. J. Chang and G. Grass, *Appl Environ Microbiol*, 2011, **77**, 794-802.
7. M. L. Knetsch and L. H. Koole, *Polymers*, 2011, **3**, 340-366.
8. Q. Yu, Y. Zhang, H. Wang, J. Brash and H. Chen, *Acta Biomaterialia*, 2011, **7**, 1550-1557.
9. D. Duday, C. Vreuls, M. Moreno, G. Frache, N. D. Boscher, G. Zocchi, C. Archambeau, C. Van de Weerdt, J. Martial and P. Choquet, *Surf Coat Tech*, 2013, **218**, 152-161.
10. F. Costa, I. F. Carvalho, R. C. Montelaro, P. Gomes and M. C. L. Martins, *Acta Biomater*, 2011, **7**, 1431-1440.
11. C. Vreuls, G. Zocchi, B. Thierry, G. Garitte, S. S. Griesser, C. Archambeau, C. Van de Weerdt, J. Martial and H. Griesser, *J Mater Chem* 2010, **20**, 8092-8098.
12. M. N. Dickson, E. I. Liang, L. A. Rodriguez, N. Vollereaux and A. F. Yee, *Biointerphases*, 2015, **10**, 021010.
13. R. E. Hancock and H.-G. Sahl, *Nature biotechnology*, 2006, **24**, 1551-1557.
14. M. Zasloff, *Nature*, 2002, **415**, 389-395.
15. J. Aveyard, M. Mehrabi, A. Cossins, H. Braven and R. Wilson, *Chem Comm*, 2007, 4251-4253.
16. L. Karam, C. Jama, P. Dhulster and N. Chihib, *J Mater Environ Sci* 2013, **4**.
17. A. A. Bahar and D. Ren, *Pharmaceuticals*, 2013, **6**, 1543-1575.
18. E. Breukink and B. de Kruijff, *Biochim Biophys Acta*, 1999, **1462**.
19. L. Karam, C. Jama, A.-S. Mamede, A. Fahs, G. Louarn, P. Dhulster and N.-E. Chihib, *React Funt Polym*, 2013, **73**, 1473-1479.

20. L. Karam, C. Jama, N. Nuns, A. S. Mamede, P. Dhulster and N. E. Chihib, *J Pept Sci*, 2013, **19**, 377-385.

21. R. Mauchauffé, M. Moreno-Couranjou, N. D. Boscher, C. Van De Weerdt, A.-S. Duwez and P. Choquet, *J Mater Chem B*, 2014, **2**, 5168.

22. A. Héquet, V. Humblot, J. Berjeaud and C. Pradier, *Colloid Surf B*, 2011, **84**.

23. L. Zhao, P. K. Chu, Y. Zhang and Z. Wu, *J Biomed Mater Res B Appl Biomater*, 2009, **91**, 470-480.

24. S. A. Onaizi and S. S. J. Leong, *Biotechnol Adv*, 2011, **29**, 67-74.

25. M. M. M. Bilek, D. V. Bax, A. Kondyurin, Y. Yin, N. J. Nosworthy, K. Fisher, A. Waterhouse, A. S. Weiss, C. G. dos Remedios and D. R. McKenzie, *Proc. Natl. Acad. Sci.* , 2011, **108**, 14405-14410.

26. M. M. Bilek and D. R. McKenzie, *Biophys Rev*, 2010, **2**, 55-65.

27. R. Barbucci, P. Torricelli, M. Fini, D. Pasqui, P. Favia, E. Sardella, R. d'Agostino and R. Giardino, *Biomaterials*, 2005, **26**, 7596-7605.

28. K. Tsougeni, P. Petrou, K. Awsiuk, M. Marzec, N. Ioannidis, V. Petrouleas, A. Tserepi, S. Kakabakos and E. Gogolides, *ACS Appl Mater Interfaces*, 2015, **7**, 14670-14681.

29. A. Conte, G. G. Buonocore, M. Sinigaglia, L. C. Lopez, P. Favia, R. d'Agostino and M. A. D. Nobile, *J Food Prot*, 2008, **71**, 119-125.

30. F. Khelifa, S. Ershov, Y. Habibi, R. Snyders and P. Dubois, *Chemical Reviews*, 2016, **116**, 3975-4005.

31. L. C. Lopez, R. Gristina, G. Ceccone, F. Rossi, P. Favia and R. d'Agostino, *Surf Coat Tech*, 2005, **200**, 1000-1004.

32. R. A. D'Sa, J. Raj, P. J. Dickinson, M. A. S. McMahon, D. A. McDowell and B. J. Meenan, *Journal of Materials Science: Materials in Medicine*, 2015, **26**, 1-13.

33. R. A. D'Sa, J. Raj, P. J. Dickinson, B. K. Pierscionek and B. J. Meenan, *Soft Matter*, 2011, **7**, 608-617.

34. R. A. D'Sa, J. Raj, M. A. S. McMahon, D. A. McDowell, G. A. Burke and B. J. Meenan, *J Colloid Interface Sci*, 2012, **375**, 193-202.

35. R. A. D'Sa, G. A. Burke and B. J. Meenan, *Journal of Materials Science-Materials in Medicine*, 2010, **21**, 1703-1712.

36. R. A. D'Sa and B. J. Meenan, *Langmuir*, 2010, **26**, 1894-1903.

37. C. V. Bonduelle, W. M. Lau and E. R. Gillies, *ACS Applied Materials & Interfaces*, 2011, **3**, 1740-1748.

38. S. N. Jampala, M. Sarmadi, E. B. Somers, A. C. L. Wong and F. S. Denes, *Langmuir*, 2008, **24**, 8583-8591.

39. S. Tan, G. Li, J. Shen, Y. Liu and M. Zong, *J. Appl. Polym. Sci*, 2000, **77**, 1869-1876.

40. S. Karamdoust, B. Yu, C. V. Bonduelle, Y. Liu, G. Davidson, G. Stojcevic, J. Yang, W. M. Lau and E. R. Gillies, *J Mater Chem*, 2012, **22**, 4881-4889.

41. M. Gu, J. E. Kilduff and G. Belfort, *Biomaterials*, 2012, **33**, 1261-1270.

42. O. Jun-Seok, A.-G. Yolanda and W. B. James, *J Phys D: Appl Phys*, 2011, **44**, 365202.

43. I. Horcas, R. Fernández, J. M. Gómez-Rodríguez, J. Colchero, J. Gómez-Herrero and A. M. Baro, *Review of Scientific Instruments*, 2007, **78**, 013705.

44. K. Vasilev, N. Poulter, P. Martinek and H. J. Griesser, *ACS Appl Mater Interfaces*, 2011, **3**, 4831-4836.

45. K. McKay, J. S. Oh, J. L. Walsh and J. W. Bradley, *J Phys D: Appl Phys*, 2013, **46**, 464018.

46. X. Qing, N. Anton Yu, G. Manuel Á, L. Christophe and L. Xin Pei, *Plasma Sources Sci*, 2013, **22**, 015011.

47. M. Thiyagarajan, A. Sarani and C. Nicula, *J Appl Phys*, 2013, **113**, 233302.

48. G. Socrates, *Infrared and Raman Characteristic Group Frequencies: Tables and Charts*, Wiley, 2004.

49. X. Qi, G. Poernomo, K. Wang, Y. Chen, M. B. Chan-Park, R. Xu and M. W. Chang, *Nanoscale*, 2011, **3**, 1874-1880.

50. R. A. D'Sa, G. A. Burke and B. J. Meenan, *Acta Biomater*, 2010, **6**, 2609-2620.

51. L. J. Harris, H. P. Fleming and T. R. Klaenhammer, *J Food Prot*, 1991, **54**.

52. G. E. Mohamed, A. Seaman and M. Woodbine, Food antibiotic nisin: comparative effects on *Erysipelothrix and Listeria* in *Antimicrobials and Agriculture*, ed. M. Woodbine, Butterworths, London, 1984, pp. 435-442.

53. A. Hurst, Nisin and other inhibitory substances from lactic acid bacteria in *Antimicrobials in foods*, eds. A. Branen and P. Davidson, Marcel Dekker, New York, 1983, pp. 327-351.

54. M. Lakamraju, J. McGuire and M. Daeschel, *J Colloid Interface Sci*, 1996, **178**, 495-504.

55. C. K. Bower, J. McGuire and M. Daeschel, *J Ind Microbiol*, 1995, **15**.

56. A. Kondyurin, P. Naseri, K. Fisher, D. R. McKenzie and M. M. M. Bilek, *Polym Degrad Stab*, 2009, **94**, 638-646.

57. K. S. Siow, L. Britcher, S. Kumar and H. J. Griesser, *Plasma Process Polym*, 2006, **3**, 392-418.

58. D. V. Bax, Y. Wang, Z. Li, P. K. Maitz, D. R. McKenzie, M. M. Bilek and A. S. Weiss, *Biomaterials*, 2011, **32**, 5100-5111.

59. Y. Yin, K. Fisher, N. J. Nosworthy, D. Bax, S. Rubanov, B. Gong, A. S. Weiss, D. R. McKenzie and M. M. M. Bilek, *Plasma Process Polym*, 2009, **6**, 658-666.

60. A. Tserepi, E. Gogolides, A. Bourkoula, A. Kanioura, G. Kokkoris, P. S. Petrou and S. E. Kakabakos, *Plasma Chem Plasma P*, 2016, **36**, 107-120.

61. P. Favia, A. Milella, L. Iacobelli and R. d'Agostino, in *Plasma processes and polymers*, eds. R. d'Agostino, P. Favia, M. R. Wertheimer and C. Oehr, Wiley-VCH, New York, 2005., pp. 271-280.

62. N. Nakajima and Y. Ikada, *Bioconjug Chem*, 1995, **6**, 123-130.

63. B. R. Coad, M. Jasieniak, S. S. Griesser and H. J. Griesser, *Surf Coat Tech*, 2013, **233**, 169-177.